

781 Mbit/s photon-counting optical communications using a superconducting nanowire detector

Bryan S. Robinson, Andrew J. Kerman, Eric A. Dauler, Richard J. Barron, David O. Caplan, Mark L. Stevens, John J. Carney, and Scott A. Hamilton

MIT Lincoln Laboratory, Lexington, Massachusetts 02420

Joel K. W. Yang and Karl K. Berggren

Department of Electrical Engineering and Computer Science, Massachusetts Institute of Technology, Cambridge, Massachusetts 02139

Received September 13, 2005; revised November 9, 2005; accepted November 10, 2005; posted November 15, 2005 (Doc. ID 64766)

We demonstrate 1550 nm photon-counting optical communications with a NbN-nanowire superconducting single-photon detector. Source data are encoded with a rate-1/2 forward-error correcting code and transmitted by use of 32-ary pulse-position modulation at 5 and 10 GHz slot rates. Error-free performance is obtained with ~ 0.5 detected photon per source bit at a source data rate of 781 Mbits/s. To the best of our knowledge, this is the highest reported data rate for a photon-counting receiver. © 2006 Optical Society of America
OCIS codes: 040.0040, 040.5570, 060.4080, 060.4510, 160.1890.

Photon-counting detectors may be employed in optical communications links to reduce receiver complexity and improve receiver sensitivity.¹ However, to date these detection techniques have not been widely used, largely because available photon-counting detectors at typical telecommunication wavelengths (1.3–1.55 μm), such as photomultiplier tubes and In-GaAs avalanche photodiodes, suffer from poor detection efficiencies, low count rates, or high dark-count rates. Previous photon-counting communications demonstrations were limited to data rates of < 500 kbits/s.^{2–4} Recently, high-speed NbN-nanowire superconducting single-photon detectors (SSPDs) capable of operating at gigahertz count rates⁵ with kilohertz dark-count rates⁶ were developed. These devices have the potential to make high-data-rate photon-counting optical communications practical.

The NbN-nanowire SSPD consists of a thin film (approximately 3–5 nm) of NbN deposited on a sapphire substrate.⁷ The film is patterned by *e*-beam lithography to form a meander-type superconducting wire of ~ 100 nm width.⁸ These wires are superconducting at temperatures below ~ 10 K. When the device is used as a single-photon detector, the wire is cooled to 2–4 K and biased with a current slightly below the critical current above which the device ceases to be a superconductor. When an incident photon is absorbed by the detector, it creates a region of increased resistance in the wire.^{6,9} The consequent decrease in the current passed by the wire may be sensed to detect the photon event. Note that the probability of detecting an incident photon increases for bias currents closer to the critical current.⁶

When these devices are used for high-data-rate optical communications (> 100 Mbits/s), a number of characteristics of the device must be taken into account. First, timing jitter in the detection process limits the temporal resolution of photon-arrival-time measurements. The timing jitter of NbN-nanowire

SSPDs was previously measured⁵ to be < 35 ps but may depend on details of the device's geometry. This jitter leads to significant intersymbol interference for data transmission slot rates of ≥ 10 GHz. Second, the recovery time for the detection process limits the maximum possible count rate of the detector. Recent measurements have shown that the minimum time between detection events in large-area SSPDs with high detection efficiencies is limited to a few nanoseconds because of the kinetic inductance of the NbN nanowire.¹⁰ Thus, photons arriving within a few nanoseconds of a previous detection event will be undetected, or blocked. Consequently, for data transmission slot rates of ≥ 1 GHz the SSPD can provide no more than one detection event per slot. In this regime of operation it is not possible to distinguish detection events arising from an incident optical pulse from those that are due to background or dark counts, even at high signal-to-noise ratios. Additionally, at high slot rates the detection of an incident signal pulse may prevent detection of subsequent pulses arriving within a few nanoseconds of the first pulse. These detection characteristics could limit the performance of links that employ NbN-nanowire SSPDs using conventional communication techniques.

To overcome these effects, we use *M*-ary pulse-position modulation (PPM) and forward-error correcting (FEC) codes. With PPM, a symbol representing $\log_2 M$ bits of information is transmitted by a single pulse sent in one of *M* transmission slots. PPM has been shown to achieve near-optimal performance, in terms of the required number of received photons per transmitted bit, for a photon-counting channel, especially for large *M*.¹ Moreover, PPM is a particularly advantageous modulation format for use with a photon counter with a limited count rate because multiple bits of information can be conveyed for each detection event, thus enabling communication at data rates higher than the maximum count

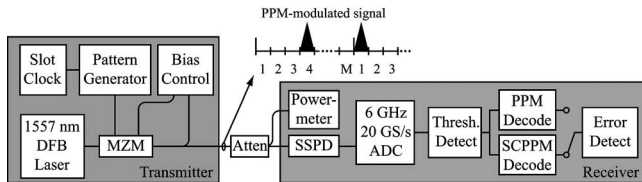


Fig. 1. Schematic diagram of experimental setup for demonstrating optical communications that use NbN-nanowire SSPDs.

rate of the detector. FEC codes are employed to overcome the effects of dark counts and blocking during detection. The FEC code used in this work was a rate-1/2 serially concatenated pulse-position modulation (SCPPM) turbo code¹¹ that comprised a rate-1/2 convolutional outer code, a 15,120 bit interleaver, and a rate-1 accumulator-PPM modulator. The code was decoded with an iterative soft-input soft-output decoder. This code was developed for a deep-space photon-counting optical communications application and has demonstrated performance within approximately 1 to 1.5 dB of the theoretical optimum channel efficiencies for these types of channel.^{4,11}

The experimental setup for demonstrating optical communications with the SSPD is shown in Fig. 1. A 1557 nm distributed-feedback (DFB) source laser was modulated with a 32-ary PPM waveform by a high-extinction Mach-Zehnder intensity modulator (MZM).¹² With 32-ary PPM, each detection event can convey as many as 5 bits of information. The pattern generator was programmed to transmit FEC-encoded PPM blocks. The attenuated optical power was measured at the receiver input by a powermeter calibrated to report the power incident on the SSPD (including a measured loss of 10 dB due to coupling optics). The SSPD used in these experiments was a $3\ \mu\text{m} \times 3.3\ \mu\text{m}$ meander with a 50% fill factor. Electrical and optical coupling to the detector have been described in Ref. 10. The detection efficiency of this device was 6.3% at a bias current of 95% of the device critical current. The time required after a detection event for the detection efficiency of the SSPD to recover to 90% of its steady-state value was measured to be 3.5 ns. The amplified electrical signal from the output of the detector was digitized by a 20 Gsample/s analog-to-digital converter (ADC) with 6 GHz analog bandwidth. Synchronization between the transmitter slot clock and the receiver sampling clock was maintained with a 100 MHz electrical reference signal between the transmitter and the receiver. Photon-arrival times were determined by detection of threshold crossings at the output of the digitizer. These arrival times could be passed either to a PPM decoder, for evaluation of the uncoded performance of the link, or to a software SCPPM decoder, for evaluation of the link performance with the FEC code.

We demonstrated receiver functionality at slot rates of 5 and 10 GHz, corresponding to uncoded (coded) data rates of 781 s (390) and 1562 (781) Mb/s, respectively, for 32-ary PPM modulation. The SSPD was cooled to 2 K and biased with a current of $18.87\ \mu\text{A}$ for operation at the 5 GHz slot rate. At 10 GHz, the SSPD was biased with a current of

$16.95\ \mu\text{A}$ in order to maintain the superconductivity of the SSPD with the increased rate of detection events. This led to a lower detection efficiency at the higher slot rate. These bias currents at the 5 and 10 GHz slot rates represent 88% and 79%, respectively, of the unilluminated SSPD critical current of $21.48\ \mu\text{A}$. The dark-count rates for these bias conditions, measured when the SSPD was not illuminated, were 8.06 and 1.44 kHz.

The incident power on the detector, P_{inc} , in units of photons per pulse, is related to the measured average power at the receiver input, P_{avg} , by $P_{\text{inc}} = P_{\text{avg}} T_{\text{sym}} / E_{\gamma}$, where T_{sym} is the symbol duration ($=M/f_s$) and E_{γ} is the photon energy. Similarly, we define the detected power, P_{det} , in units of photons per pulse, in terms of the measured probability of a detection event in slots containing an incident pulse, p_d , as $P_{\text{det}} = -\ln(1 - p_d)$. Figure 2 shows the measured detected power as a function of the incident power for a 32-ary PPM-modulated signal at 5 and 10 GHz slot rates. The system detection efficiency of the SSPD receiver, including both the device detection efficiency and the blocking losses, is simply $P_{\text{det}}/P_{\text{inc}}$. At 5 GHz the measured system detection efficiency is $\sim 3\%$ at low incident powers. At higher intensities the detection efficiency improves to $\sim 5\%$. We also observed an increase in the dark-count rate of the detector, as well as a decrease in the critical current of the detector, at higher incident intensities. These effects may be due to detector heating as the count rate of the detector increases. The effects are even more pronounced at 10 GHz, where the incident pulse rate is doubled. At low intensities, a detection efficiency of 0.5% is observed due to the lower bias current in the 10 GHz measurement. As the incident power is increased, the detection efficiency improves to $\sim 2.8\%$. The effect of detector blocking between detection events manifests itself as a saturation in the detected power at high incident powers. As expected, this saturation occurs at a lower detected power at the 10 GHz slot rate owing to the increased blocking probability of the detector at higher pulse rates.

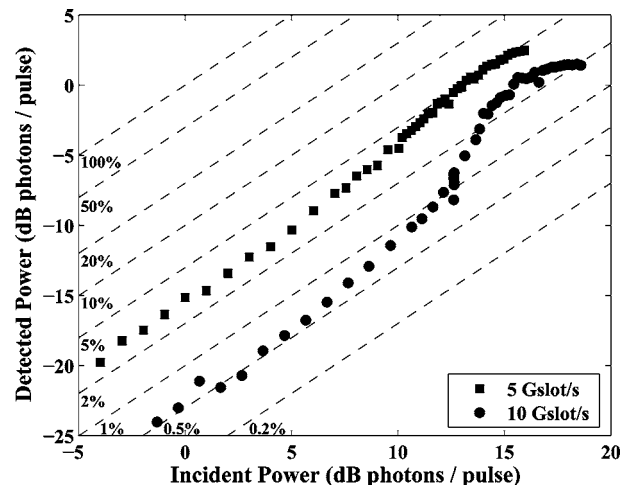


Fig. 2. Intensity-dependent detection characteristics of the SSPD in response to a 32-ary PPM signal at 5 and 10 GHz slot rates. Dashed lines, curves of constant detection efficiency.

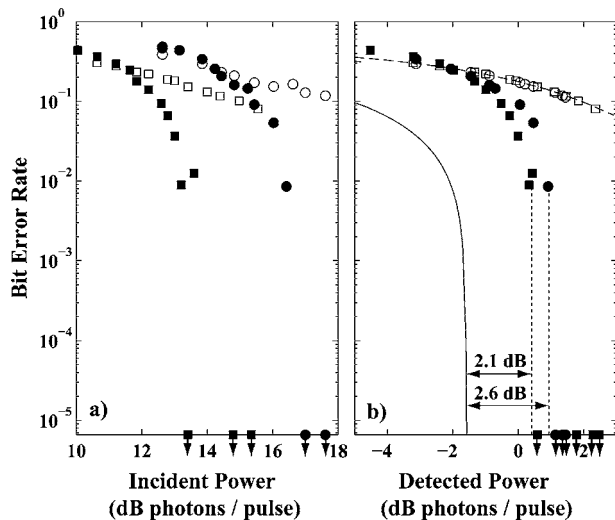


Fig. 3. Measured uncoded (open symbols) and coded (filled symbols) bit-error-rate performance at 5 (squares) and 10 (circles) GHz slot rates versus incident and detected power. Dashed lines, theoretical uncoded bit-error-rate performance for a Poisson channel. Solid curve, theoretical optimum performance for a background-free 32-ary PPM erasure channel with Poisson statistics.

Figure 3 shows the measured communications performance of the SSPD receiver operating at 5 and 10 GHz slot rates. As expected from the detection efficiency measurements, the uncoded performance saturates at a bit-error rate of $\sim 10^{-1}$ owing to the inductance-limited detector blocking. However, once the detection efficiency is accounted for and the performance is plotted as a function of the detected power, we find good agreement between the measured data and the theoretical performance of a background-free Poisson channel. When the SCPPM FEC code is used, error-free performance is obtained for detected powers in excess of 0.6 dB photons per pulse at 5 GHz and 1.1 dB photons per pulse at 10 GHz, which represent penalties of 2.1 and 2.6 dB from the theoretical optimum performance for an ideal memoryless photon-counting channel with this modulation format. The additional 0.5 dB performance penalty observed at the 10 GHz slot rate is due to increased detector blocking as well as to intersymbol interference that arises from bandwidth limitations in the transmitter and receiver and jitter from the SSPD. With the rate-1/2 FEC code, each pulse (representing a single 32-ary PPM symbol) conveys 2.5 bits of information. Thus the demonstrated receiver efficiency is 2.2 bits per detected photon at a 5 GHz slot rate and 1.9 bits per detected photon at a 10 GHz slot rate.

In summary, we have demonstrated the use of high-speed NbN-nanowire SSPDs for high-data-rate photon-counting optical communications. While the detection efficiency of the device used in these experiments was limited to $\leq 5\%$, we used a rate-1/2 SCPPM FEC code to demonstrate receiver efficien-

cies of 1.9–2.2 bits per detected photon (8–20 incident photons per bit). Error-free communications performance was obtained for slot rates as high as 10 GHz, corresponding to a source data rate of 781 Mbits/s. This is more than a 1000-fold improvement over previously reported results with a photon-counting optical receiver.

We are grateful to G. Gol'tsman and B. Voronov (Moscow State Pedagogical University) for providing the NbN thin films used in this work and R. Sobolewski (University of Rochester) for helpful discussions and technical assistance. This research is sponsored by the U.S. Air Force under contract #FA8721-05-C-0002. Opinions, interpretations, recommendations, and conclusions are those of the authors and are not necessarily endorsed by the U.S. Government. B. Robinson's e-mail address is brobinson@ll.mit.edu.

References

1. J. R. Pierce, *IEEE Trans. Commun.* **COM-26**, 1819 (1978).
2. J. Katz, TDA Progress Report 42-70 (Jet Propulsion Laboratory, California Institute of Technology, 1982), p. 95, http://tmo.jpl.nasa.gov/ipn_progress_report/tda.cfm.
3. K. J. Gordon, V. Fernandez, P. D. Townsend, and G. S. Buller, *IEEE J. Quantum Electron.* **40**, 900 (2004).
4. B. S. Robinson, D. O. Caplan, M. L. Stevens, R. J. Barron, E. A. Dauler, and S. A. Hamilton, in *2005 Digest of the LEOS Summer Topical Meetings* (IEEE, 2005), paper TuA3.1.
5. J. Zhang, W. Slysz, A. Verevkin, O. Okunev, G. Chulkova, A. Korneev, A. Lipatov, G. N. Gol'tsman, and R. Sobolewski, *IEEE Trans. Appl. Supercond.* **13**, 180 (2003).
6. G. N. Gol'tsman, O. Okunev, G. Chulkova, A. L. A. Semenov, K. Smirnov, B. Voronov, A. Dsardanov, C. Williams, and R. Sobolewski, *Appl. Phys. Lett.* **79**, 705 (2001).
7. S. Cherednichenko, P. Yahoubov, K. Il'in, G. Gol'tsman, and E. Gershenson, in *Proceedings of the Eighth International Symposium on Space Terahertz Technology* (Harvard U., 1997), p. 245.
8. J. K. W. Yang, E. Dauler, A. Ferri, A. Pearlman, A. Verevkin, G. Gol'tsman, B. Voronov, R. Sobolewski, W. E. Keicher, and K. K. Berggren, *IEEE Trans. Appl. Supercond.* **15**, 626 (2005).
9. A. M. Kadin and M. W. Johnson, *Appl. Phys. Lett.* **69**, 3938 (1996).
10. A. J. Kerman, E. A. Dauler, W. E. Keicher, J. K. W. Yang, K. K. Berggren, G. Gol'tsman, and B. Voronov, "Kinetic-inductance-limited reset time of superconducting nanowire photon counters," arXiv.org print/archive physics/0510238 (October 26, 2005).
11. B. E. Moision and J. Hamkins, Interplanetary Network Progress Report 42-161 (Jet Propulsion Laboratory, California Institute of Technology, 2005), p. 1, http://tmo.jpl.nasa.gov/ipn_progress_report/ipn.cfm.
12. D. O. Caplan, B. S. Robinson, R. J. Murphy, and M. L. Stevens, in *Optical Fiber Communications Conference 2005* (Optical Society of America, 2005), paper PDP32.